

Supporting Information for:

Towards Organic Energy Storage: Characterization of 2,5-bis(methylthio)thieno[3,2-b]thiophene

Stephen E. Burkhardt^a, Sean Conte^a, Gabriel G. Rodriguez-Calero^a, Michael A. Lowe^a,
Hualei Qian^a, Weidong Zhou^a, Jie Gao^a, Richard G. Hennig^b, Héctor D. Abruña^{a*}

^aDepartment of Chemistry and Chemical Biology,

Baker Laboratory, Cornell University, Ithaca, New York 14853-1301, USA

^bDepartment of Materials Science and Engineering,

Bard Hall, Cornell University, Ithaca, New York 14853-1501, USA

Email: hda1@cornell.edu

Table S1. Binding energies for dimer species of **2** using the 6-31+G(d,p) basis set.

Species	6-311++g(d,p) Binding Energy (eV)	6-31+G(d,p) Binding Energy (eV)	Reference
D1+	0.086058774	0.102404662	vs. M ¹⁺ + M ⁰
D2+	0.270490296	0.321259693	vs. M ¹⁺ + M ¹⁺
D2+	-0.893241689	-0.857538155	vs. M ²⁺ + M ⁰
D3+	0.091241729	0.092141066	vs. M ²⁺ + M ¹⁺

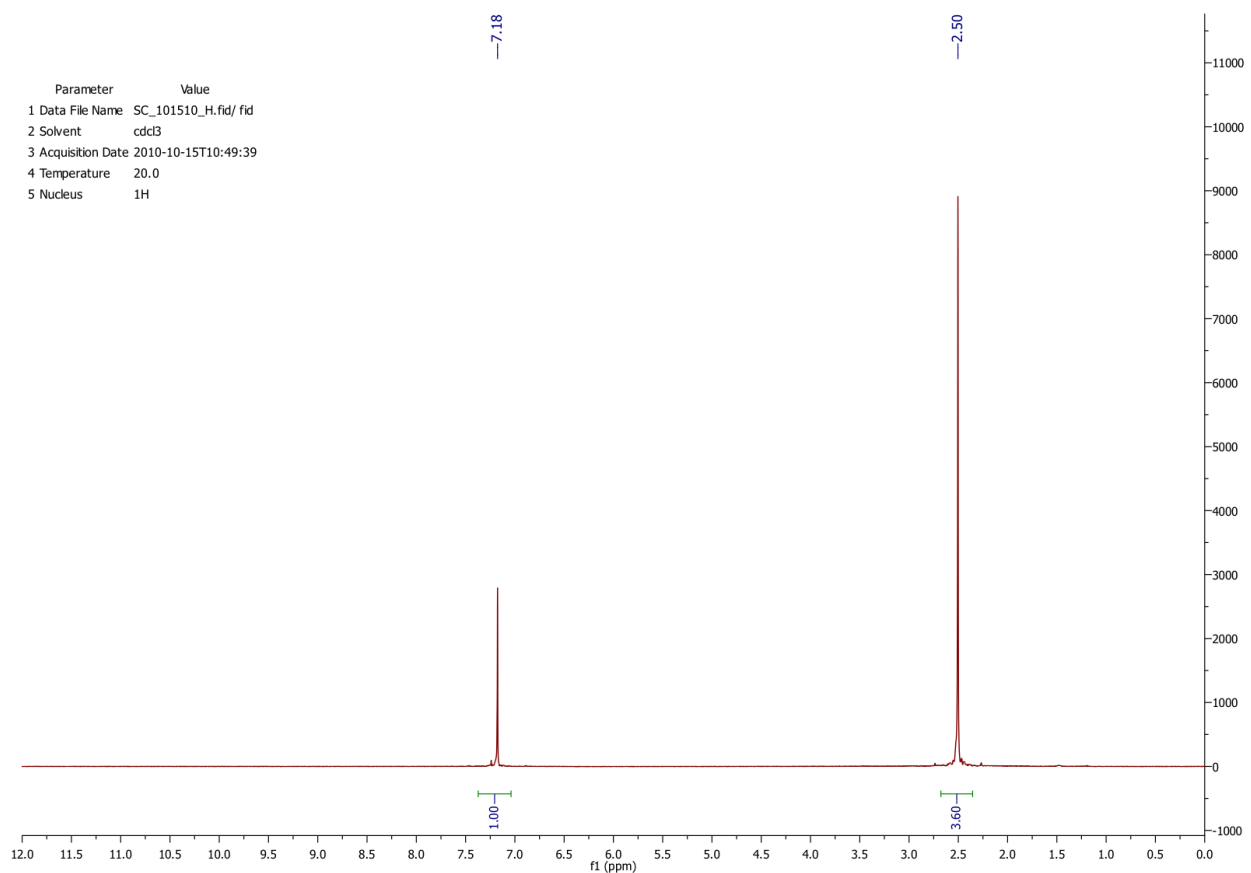


Figure S1. Proton NMR for **2**. Chemical shifts are identical to those previously reported.

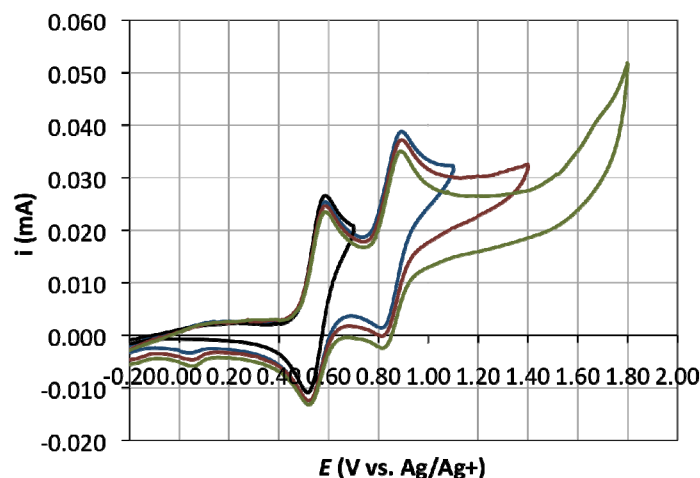


Figure S2. a.) Window opening cyclic voltammetry showing reverse potentials at 700, 1100, 1400 and 1800 mV respectively.

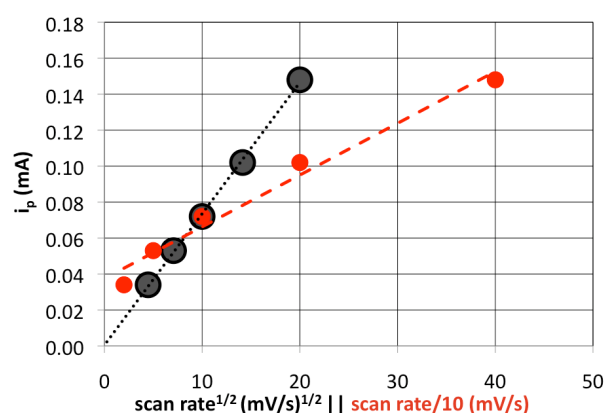


Figure S3. Plots of peak current vs. scan rate (red), and the square root of the scan rate (black) for the first oxidation of a 1mM solution of **2**. The linear relationship between the peak current and the square root of the scan rate characterizes the electrode process as diffusional.

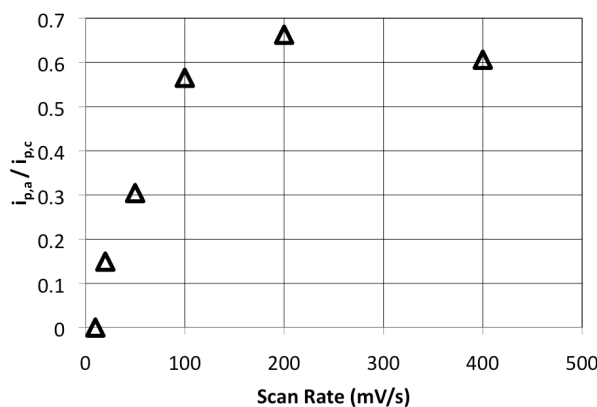


Figure S4. Plot of $i_{p,a}/i_{p,c}$ vs. scan rate for the reduction process at +100mV. The reversibility of the peak appears to increase as the scan rate gets faster, implying an EC mechanism. Note that the reduction peak also shrinks with scan rates greater than ~100mV. In the case of the 400 mV/s peak, subtraction of the base line is very difficult and this point may have a large degree of error.

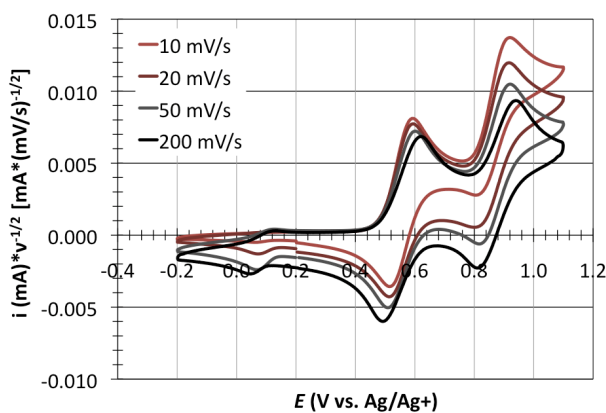


Figure S5. CVs of a 1mM solution of **2** normalized to the square root of the scan rate. The increase in normalized current, along with the positive shift in potential in the second oxidation wave, implies an ECE or EC_{cat} mechanism, consistent with RDE results.

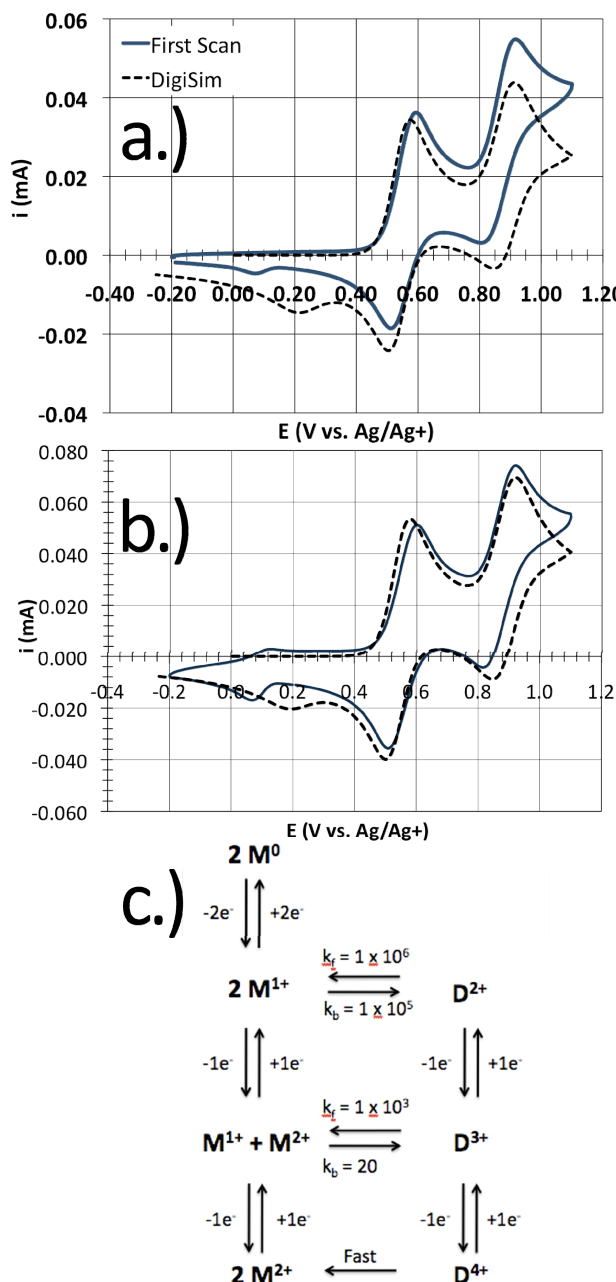


Figure S6. a.) Experimental (solid) and DigiSim (dashed) cyclic voltammetry at 20mV/s
b.) Experimental (solid) and DigiSim (dashed) cyclic voltammetry at 50mV/s. c.)
Proposed mechanism and equilibrium details used for DigiSim simulations.

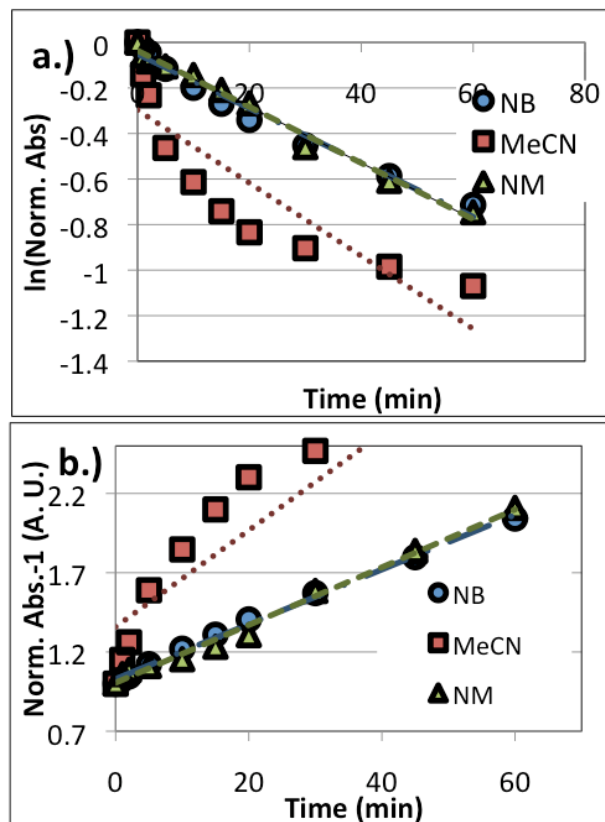


Figure S7. Plots of a.) natural log of the absorbance vs. time and b.) absorbance-1 vs. time. All of these plots deviate from linearity. No conclusions can be made regarding the order of the radical cation “self-discharge” reaction from this data.

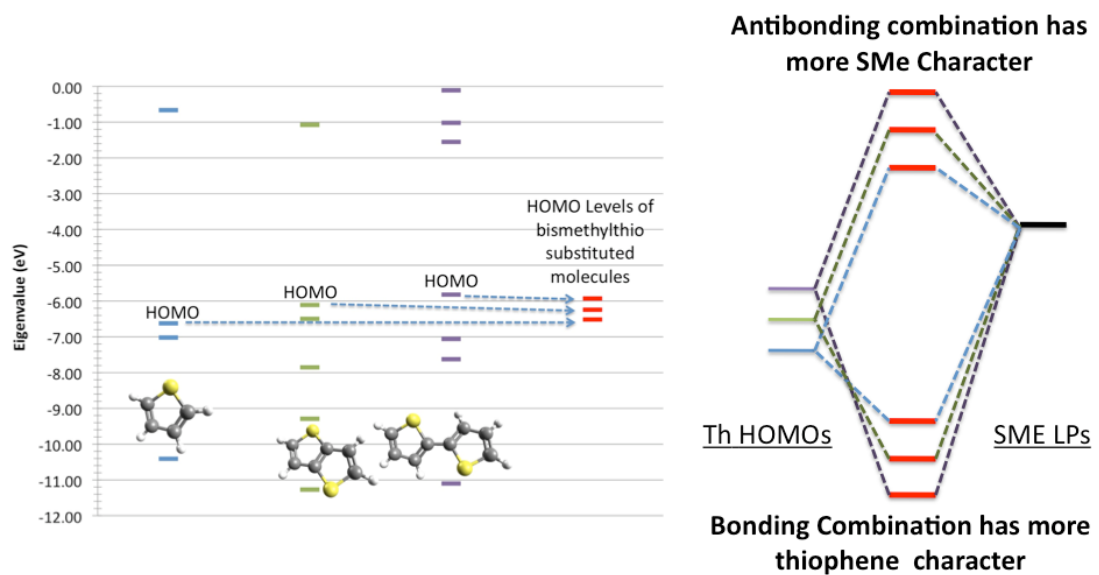


Figure S8. Calculated HOMO levels for thiophenic fragments and schematic MO diagram of the interaction between the thioether lone pairs and the HOMO (π -type) of the

thiophenic core. The MO diagram explains why the larger conjugated chains appear to have more evenly distributed spin density.

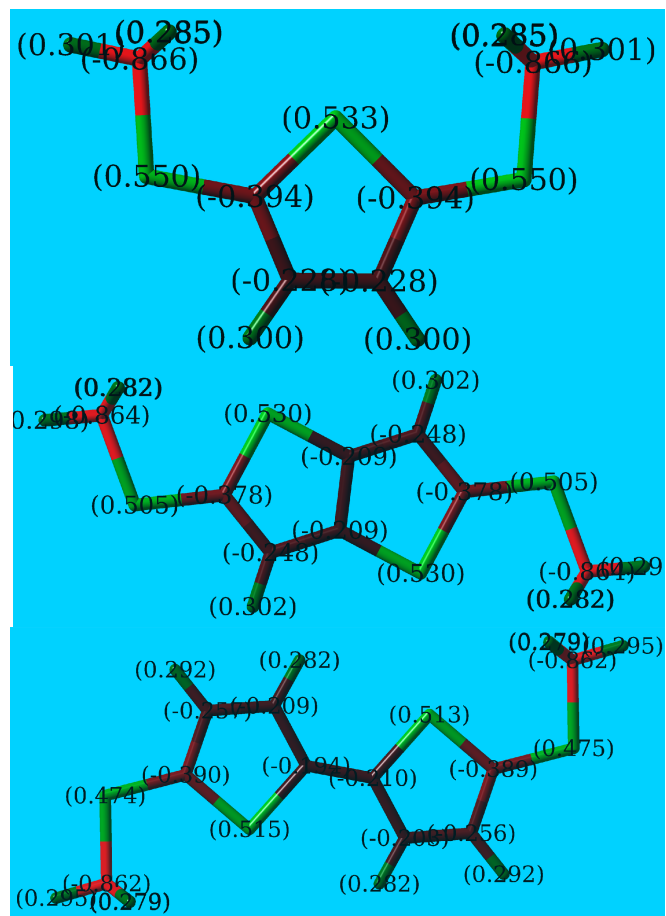


Figure S9. NBO calculated charges for radical cations of **1**, **2** and **3**. In all cases, the thioether sulfur bears the most positive charge, consistent with oxidation of the sulfur lone pairs.

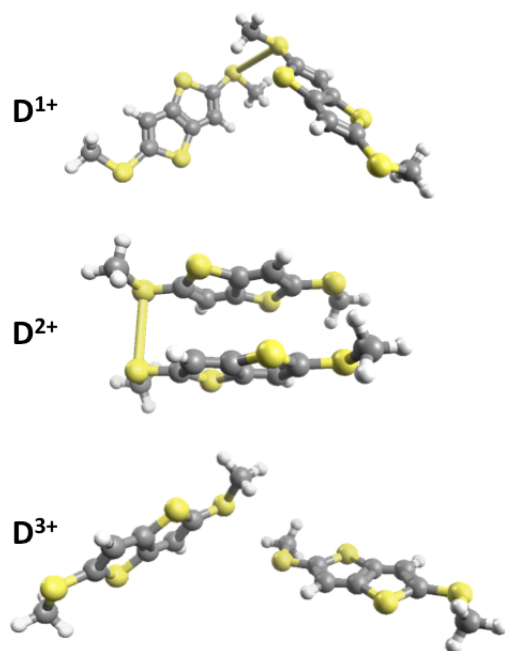


Figure S10. Computationally predicted dimer geometries for D^{1+} , D^{2+} , D^{3+} . In all cases there appears to be a significant interaction between thioether sulfurs. Similar interactions have been observed in oxidized aliphatic thioethers. Images were produced using Avogadro, and bonds between sulfur atoms were determined by default parameters of the program.

Complete References:

30. Gaussian 03, Revision E.01,
M. J. Frisch, G. W. Trucks, H. B. Schlegel, G. E. Scuseria,
M. A. Robb, J. R. Cheeseman, J. A. Montgomery, Jr., T. Vreven,
K. N. Kudin, J. C. Burant, J. M. Millam, S. S. Iyengar, J. Tomasi,
V. Barone, B. Mennucci, M. Cossi, G. Scalmani, N. Rega,
G. A. Petersson, H. Nakatsuji, M. Hada, M. Ehara, K. Toyota,
R. Fukuda, J. Hasegawa, M. Ishida, T. Nakajima, Y. Honda, O. Kitao,
H. Nakai, M. Klene, X. Li, J. E. Knox, H. P. Hratchian, J. B. Cross,
V. Bakken, C. Adamo, J. Jaramillo, R. Gomperts, R. E. Stratmann,
O. Yazyev, A. J. Austin, R. Cammi, C. Pomelli, J. W. Ochterski,
P. Y. Ayala, K. Morokuma, G. A. Voth, P. Salvador, J. J. Dannenberg,
V. G. Zakrzewski, S. Dapprich, A. D. Daniels, M. C. Strain,
O. Farkas, D. K. Malick, A. D. Rabuck, K. Raghavachari,
J. B. Foresman, J. V. Ortiz, Q. Cui, A. G. Baboul, S. Clifford,
J. Cioslowski, B. B. Stefanov, G. Liu, A. Liashenko, P. Piskorz,
I. Komaromi, R. L. Martin, D. J. Fox, T. Keith, M. A. Al-Laham,
C. Y. Peng, A. Nanayakkara, M. Challacombe, P. M. W. Gill,
B. Johnson, W. Chen, M. W. Wong, C. Gonzalez, and J. A. Pople,
Gaussian, Inc., Wallingford CT, 2004.